Radiation Measurements 171 (2024) 107065

Contents lists available at ScienceDirect

Radiation Measurements

journal homepage: www.elsevier.com/locate/radmeas

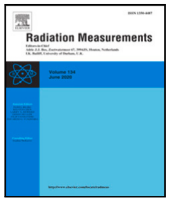

Long-term field studies of a distributed network of sensors for environmental radiological monitoring

N. Heracleous [a,*], K. Bauer [a], L. Gallego Manzano [a,c], F. Murtas [b,1], M. Silari [a], L. Svihrova [a,d]

[a] CERN, 1211 Geneva 23, Switzerland
[b] Frascati National Laboratories, INFN, 00044 Frascati, Italy
[c] Institute of Radiation Physics, Lausanne University Hospital, 1007 Lausanne, Switzerland
[d] Faculty of Nuclear Sciences and Physical Engineering, Czech Technical University, Prague 115 19, Czech Republic

ARTICLE INFO

Keywords:
Radiation
Environmental monitoring
Radioactive waste monitoring
Data analysis
LoRa
Internet of Things

ABSTRACT

The W-MON project goal is to establish an automatic control mechanism of the presence of radioactive material in conventional waste containers at CERN using a distributed network of interconnected low-power radiation sensors. This network facilitates continuous data recording, transfer and storage in a database while allowing online and offline data analysis, in addition to alarm triggering. Data transmission, processing and evaluation is achieved by a centralized IoT end-to-end data architecture that has been developed for real-time monitoring and visualization of the radiation levels in waste containers. In this paper the results of field tests of the W-MON system described in two previous papers are presented for three different types of sensors. Estimation of failure detection probability, long-term stability tests and sensitivity studies carried out using radioactive samples of various activities placed in standard waste containers are described. A comparison between the manual monitoring procedure currently used at CERN and the W-MON system is discussed in detail.

1. Introduction

CERN operates a complex and extended system of radiation monitors to ensure the safety of its personnel, its accelerators and experimental apparatus, as well as to protect the environment. In addition to this monitoring system, multi-level radiological controls of about 200 household containers for ordinary waste are routinely performed to prevent the potential accidental release of radioactive material outside CERN. The first-level controls are performed manually by radiation protection technicians with hand-held radiation survey meters (Section 2.2), every two to three days prior to the final disposal of the waste from the CERN sites. The radiation to be monitored is gamma rays, with sensitivity down to the natural background level (of the order of 0.1 μSv/h). The Waste radiation MONitoring (W-MON) system has been designed and prototyped to automatize these controls, employing a distributed Internet of Things (IoT) network of small, smart, interconnected low-power radiation detectors. The key development is the integration of lightweight but sensitive radiation sensors in a network allowing continuous data recording, transfer and storage in a database for monitoring, data analysis and alarm triggering. This system is meant to replace the current burdensome and taxing job of manual controls and aims to overcome limitations such as gaps in sensitivity, lack of time-stamped measurements, weakness in tracking potential incidents, and absence of automatic data acquisition, recording and analysis.

The technical features of W-MON have been extensively described in two previous papers. The first (Gallego Manzano et al., 2020) provided a thorough overview of the key aspects of the project, illustrated its technical details, presented the proof of concept of the system demonstrating its technology capabilities, introduced the developments of a customized solution for the radiation sensors and reported on the results of laboratory tests. The second paper (Gallego Manzano et al., 2021) provided a detailed description of the W-MON IoT infrastructure, introducing – for the first time – the application of IoT to real-time remote monitoring of radioactivity in metallic waste containers spread over a very wide area. The proposed IoT infrastructure incorporates a low-power wide-area network (LPWAN) that uses long range (LoRa) technology, enabling a large-area low-power IoT deployment. The system follows the standards and protocols of an IoT LoRaWAN architecture, designed to cover an area of hundreds of hectares with thousands of sensors working simultaneously for several years. The previous publications have shown that the sensors provide stable low-dose-rate measurements under demanding operating conditions. The radiation levels are periodically transmitted to the LoRa

* Corresponding author.
E-mail address: natalie.heracleous@gmail.com (N. Heracleous).
[1] Deceased.

https://doi.org/10.1016/j.radmeas.2024.107065
Received 3 September 2023; Received in revised form 8 December 2023; Accepted 22 January 2024
Available online 23 January 2024

server and stored in a database with a detailed event log. A set of web-based user applications with graphic controls for real-time data visualization have been designed based on open-source tools. The IoT end-to-end data infrastructure has been tested for over a year showing stable and reliable operation. Before moving to the final integration of W-MON into the overall CERN Radiation and Environment Monitoring Unified Supervision service (REMUS) (Ledeul et al., 2015), tests under real operational conditions are needed. This third and last paper presents the results of W-MON field tests carried out with three distinct types of sensors, estimating the failure detection probability, reporting the results of long-term stability tests and of sensitivity studies carried out using radioactive samples of various activities placed in standard waste containers. A comparison between the performances of the manual monitoring procedure currently used at CERN and the W-MON system is discussed in detail.

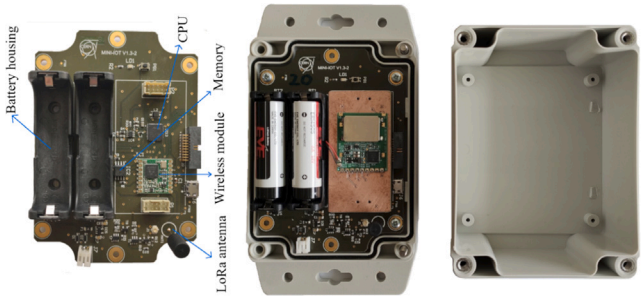

Fig. 1. Electronic board with LoRa data transmission (left) and customized D-shuttle radiation sensor connected to the communication board (center). The device is hosted in an IP67 plastic box (center and right).

2. Materials and methods

2.1. W-MON devices and network

Each of the W-MON devices includes a gamma radiation sensor with a high sensitivity down to natural background radiation level and an ultra low-power electronic board with custom-designed hardware and software, called MiniIoT board. The MiniIoT board is responsible for providing long-range low-power wireless communication using LoRa, reading/writing to flash memory, a USART interface for debugging and a monitoring system of the battery lifetime. The board includes an ATSAML21G18B micro-controller, a RFM95W-868S2 LoRa module, and an ANT-868-JJB-ST LoRa antenna. The micro-controller is programmed with custom firmware implementing the measurement cycle and logic. The devices are battery-powered by two 3.6 V, 2.6 Ah Lithium-Thionyl Chloride AA batteries. The MiniIoT board has been designed to host different sensor types. An intermediate printed circuit board (PCB) is required to connect each sensor to the communication board. Three radiation sensors are investigated as potential candidates for final use: a customized version of the D-shuttle personal dosimeter developed by the Japanese National Institute of Advanced Industrial Science and Technology (AIST) [2] in collaboration with Chiyoda Technol Corporation [3], the BG51 commercialized by the Swiss company Teviso Technologies [4] and the NI-RM02 developed by the Italian Nuclear Instruments. Throughout this document devices equipped with the three sensors will be referred to as DS, BG and NI devices respectively. The three sensors are energy efficient PIN-diode Si-based devices of different size and were calibrated and characterized before use (Gallego Manzano et al., 2020). Each end-device is housed in a IP67 plastic box for mounting in the 800 liter metallic waste containers (Fig. 1). A centralized IoT (Internet of Things) end-to-end data architecture has been developed for real-time monitoring and visualization of the radiation levels in the containers. The transmission of the data is achieved by the Low Power Wide Area Networks (LPWAN) technology via LoRa, which provides long-range low-power wireless communication (around 2 km in dense urban areas and up to 15 km in open space). Additionally, LoRa offers the possibility to serve millions of devices operating at low data rates. W-MON utilizes the CERN LPWAN network based on LoRaWAN, which operates with MQTT (Message Queuing Telemetry Transport) protocol for communication and guarantees a secure data flow across the network. The global W-MON network consists of devices, gateways, network services, a database and application servers. Studies to probe the frequency and the size of the transmitted data streams (payload) were performed taking into account the LoRa transmission efficiency and reliability, as well as information required for storage and further offline analysis. Data from each radiation sensor are transmitted every hour to the LoRaWAN Network server. The sensors record the radiation levels for a total of 57 min and use three minutes to send the data via LoRa. More specifically, each one-hour period consists of three measurement periods of 19 min. After each period, one minute is used for storing the value locally and transmitting an alarm if needed (3 × (19+1) min). The measurements are stored in an on-board flash memory, so that in case of a LoRa network failure the data are backed up for at least three hours. The payload size is fixed at 41 bytes with 30 bytes of sensor data. More information are given in a previous paper (Gallego Manzano et al., 2021).

The data is collected and stored in a centralized database system provided by CERN, based on Kafka[5] for real-time data streaming and InfluxDB[6] for data storage. A set of customized user dashboards was created using Grafana[7] for real-time monitoring, data visualization, and status control of the devices. Grafana is a visualization platform that allows designing interactive dashboards to query, visualize, and define levels of alerts on metrics and logs. The new W-MON data infrastructure is a reliable and highly scalable monitoring architecture, designed to ensure and facilitate the final integration of the system into REMUS, CERN's radiation supervisory system. Details on the communication technology used for W-MON are given elsewhere (Gallego Manzano et al., 2021).

The on-the-field operational tests performed over a period of several months discussed in this paper had the objective to compare the performance of the three types of sensors in an operational scenario. Factors such as sensitivity (which is comparable for the three sensors in terms of count rate normalized to sensor surface) and reliability, but also cost-effectiveness, scalability, long-term component availability, power consumption and lifetime expectancy are key parameters for the final design of a full-scale W-MON system (Gallego Manzano et al., 2020).

2.2. Manual monitoring procedure

The survey meters mostly used at CERN to manually search for radioactive sources and for radiological monitoring of radioactive materials, components or waste that may have been activated in the accelerator tunnels or in the experimental areas, employ Bismuth Germanate scintillator (BGO) detectors. The commercial device currently employed for ambient dose equivalent rate, H*(10), measurements is the Thermo Fischer digital survey meter FH40 [8] coupled with a

[2] https://www.aist.go.jp/index_en.html
[3] https://www.c-technol.co.jp/eng
[4] https://www.teviso.com/file/pdf/bg51-data-specification.pdf

[5] https://kafka.apache.org
[6] https://www.influxdata.com
[7] https://grafana.com
[8] https://www.thermofisher.com/order/catalog/product/FH40GLDS3?SID=srch-srp-FH40GLDS3

FHZ512 BGO probe, a 1.5 in × 1.5 in scintillator plus photomultiplier tube, allowing highly sensitive and integral measurements of gamma radiation.

These detectors are being used during the weekly controls that the radiation protection technicians perform by scanning around the metallic containers for conventional waste, checking the background and radiation levels. All tests performed with the W-MON system described in this paper were also performed using a BGO survey meter for direct comparison.

2.3. Operating environment and topology

The waste containers are located outdoors, exposed to variable weather conditions and broad temperature changes, and emptied two to three times per week via the standard garbage collection procedure that implies flipping them over with severe vibrations and shocks. A full-scale W-MON system would consist of nearly 2000 sensor units placed in about 200 containers located within the CERN sites (extending over hundreds of hectares).

The sensitivity of the W-MON system is the most important factor that essentially determines the feasibility of this project. A crucial parameter affecting the sensitivity is the distance between the radiation source and the sensor. For a point source, the intensity of the radiation field decreases with the square of the distance from the source. This was taken into account when choosing the number, location and distance between the devices in the container. The minimum number of sensors and their geometrical arrangement around the container were decided based on an extensive geometrical analysis. The volume of the container was divided in cubic voxels of 5 cm × 5 cm × 5 cm, and via a raster scan a map of the distance between any point inside the container and its closest sensor was generated using Python (Van Rossum and Drake, 2009). The analysis was performed for three configurations with six, eight and ten devices per container. The goal was both to assess the suitability of the sensors to measure weakly radioactive waste and to verify their robustness and stability over extended periods of time. The study showed that at least eight sensor units are needed to ensure full coverage of the approximately 1-m^3 volume container with dimensions of 110 cm × 70 cm × 90 cm and to detect radioactivity wherever an activated piece of material may end up in the container: two on the lid, two on the bottom, and one at the center of each of the four side walls. The detectors were fixed to the inner walls of the containers, with the exception of the two positioned at the bottom, which were attached externally. This arrangement was implemented to enhance the protection of the detectors from adverse weather conditions or potential damage during the emptying process. Specifically, situating the bottom detectors externally was a preventive measure to protect it from potential water damage caused by rain or the impact of heavy objects being thrown into the container. Detailed information on geometrical configuration and number of sensors per container can be found in Gallego Manzano et al. (2020, 2021).

3. Failure detection probability

Each sensor is an independent LoRa transceiver acting as a stand-alone monitoring unit. This means that each device measures the radiation level continuously and sends the collected data to the LoRa server every hour. If one of the devices fails, the other devices are unaffected and continue to operate. We therefore make two main assumptions: there is no correlation among devices and the radioactive object is assumed to be detected if at least one of the sensors measures a count rate above a certain threshold. As a result, the probability of failure reported here is calculated per device.

The LoRa transmission efficiency is defined as the number of transmitted packets that are successfully received by the server divided by the expected number of transmissions. Assuming a gamma detection efficiency per sensor of 100%, i.e. if a radioactive material is dumped in the container at least one sensor will detect it, the detection efficiency only depends on the LoRa transmission efficiency and hence, in the following, both terms are used interchangeably.

The radiation sensors transmit the data to the supervision system every hour. In that sense, if a radioactive item is thrown in the container within the time window between the last data transmission and the garbage collection, the alarm will not be sent on time and the object will not be detected by the W-MON system. For these cases, the probability of failure is always one.[9] The probability of throwing a radioactive object in a container is assumed to be constant, *i.e.* independent of the time of the day, and the failure probability is random. The list of hypotheses used in the reported calculations is presented below:

1. All devices are independent of one another.
2. The devices are sending data every hour. Therefore, the longer the time interval between the disposal of the object and garbage collection, the lower the probability of the piece going undetected.
3. The probability of failure is random.
4. Assuming that someone throws something in the container, the probability is uniform during the time between two consecutive garbage collections, and can be expressed as:

$$P_{thrown} = \frac{1}{n} \tag{1}$$

   where n is the number of time intervals between two consecutive garbage collections.
5. The sensitivity of the sensors to gamma rays is not taken into consideration (100% gamma detection efficiency).
6. The detection probability is equal to the LoRa transmission efficiency.
7. h is the time in hours until the next garbage collection. Therefore, the hour when the track passes (or collection hour) is h = 0. One hour until the collection is h = 1, and so on.

Based on these assumptions, and considering that the garbage truck passes once per day at any time of the day to collect the waste, the estimated minimum expected failure probability for the W-MON system is:

$$\begin{aligned} P_{day} &= P_{thrown} \times \sum_{i=0}^{n} P_{failure\ at\ h=i} = \\ &= \frac{1}{n} \times \sum_{i=0}^{n} (1-\epsilon)^i = \frac{1}{24} \sum_{i=0}^{23} (1-\epsilon)^i \end{aligned} \tag{2}$$

where $(1-\epsilon)$ is the probability that an event is not detected, being ϵ the LoRa transmission efficiency. The variable i represents the number of hours until collection, denoting the number of attempts the system has to perform to successfully send a signal before the scheduled collection. Consequently, the term $(1-\epsilon)^i$ symbolizes the probability of all transmission attempts failing from the moment the object was disposed of until the collection time.

Extensive experimental tests have shown that the LoRa transmission efficiency for all devices in a waste container is close to 100% (Gallego Manzano et al., 2021). However, the packet reception ratio can be affected by numerous reasons, for instance the weather conditions (Cattani et al., 2017), (Wennerström et al., 2013), collisions or signal overlap among devices which depends on the location of the container, loss of LoRa connectivity associated to a network problem, etc. Therefore, realistically, one could assume an average detection efficiency of 80%. Taking this into account, the probability of missing a radioactive

[9] A probability of failure equal to one corresponds to the worst-case scenario. In reality, this probability should be ≤ 1 as it depends on the time the item is thrown in the container and the dose rate of the radioactive object.

object in a waste container per day assuming a random and daily garbage collection is 5%.

At CERN, garbage collection is performed two to three times per week according to a specific collection schedule. Consequently, the failure probability might decrease from 5% for a random and daily garbage collection to 2.2% or 1.4% depending on the weekly collections. It is worth mentioning that the probability of failure does not significantly change by changing the detection efficiency of the detector, being always below 5%. Even for an ideal detector, with a 100% detection efficiency and 100% LoRa transmission efficiency, the probability of failure is around 2%, which implies that it is dominated by the fact that the W-MON system is not able to send an alarm on time if the radioactive item is dumped in the container just before the collection. To overcome this limitation, the system includes a high-count rate alarm that will immediately trigger when a highly active item is dumped in the container. However, this fail-safe mechanism does not apply to low-activated objects, as they require a longer integration time to trigger the system. Nonetheless, it should be emphasized that the sensor's detection efficiency to gamma rays has not been taken into consideration and therefore, the results may vary depending on the activity, geometry, energy of emitted gamma rays and position of the radioactive objects in the container.

4. Results and discussion

4.1. Temperature tests in climate chamber

Temperature variations can greatly affect not only the electronics but also the radiation sensor itself. The W-MON devices will need to operate outdoors and unattended for extended periods of time (years), and will therefore be subjected to large temperature variations. To verify the continuous and unbiased behavior of the devices at various temperatures, tests were first performed in a climate chamber under well-controlled conditions. The measurements lasted 23 h, during which the temperature was increased from −20 °C to +50 °C. Three devices of each type (BG, NI and DS) were simultaneously placed in the chamber; additional devices were placed outside the chamber to act as a reference. All sensors demonstrated a stable behavior during the test: the number of counts was stable and within the expected uncertainty, even at the highest temperatures. The sensors continued to send meaningful data throughout the test. Fig. 2 shows the number of counts versus time and the temperature profile for the three types of sensors. In Fig. 2(c), instances of zero values become evident as the temperature approaches 50 °C, indicating a limitation in the NI sensor's functionality under extremely high temperatures. Even after a mechanical upgrade to fix the problem was implemented, the sensor still does not work perfectly at high temperatures. However, when the temperature decreases the sensor regains normal functionality, accurately measuring as intended. This shows that environmental conditions, especially temperature, are crucial for NI sensor performance.

4.2. Long term outdoors tests

A long-term, on-the-field operational test was performed with three standard containers, each equipped with eight sensors of the same type: one with DS, one with BG and one with NI devices. The test lasted for several months, from February 2021 until May 2021. The objective was to compare the performance of the three types of sensors and evaluate factors such as the sensitivity (which is similar in terms of count rate normalized to sensor surface), robustness, reliability, power consumption and lifetime expectancy of the W-MON system. The results of these tests effectively evaluate the feasibility of W-MON as an automatic monitoring system. The containers were placed in outdoor locations on the Meyrin site of CERN and routinely used for the collection of ordinary waste, treated and emptied under standard operational conditions throughout the period. The detectors were monitored via

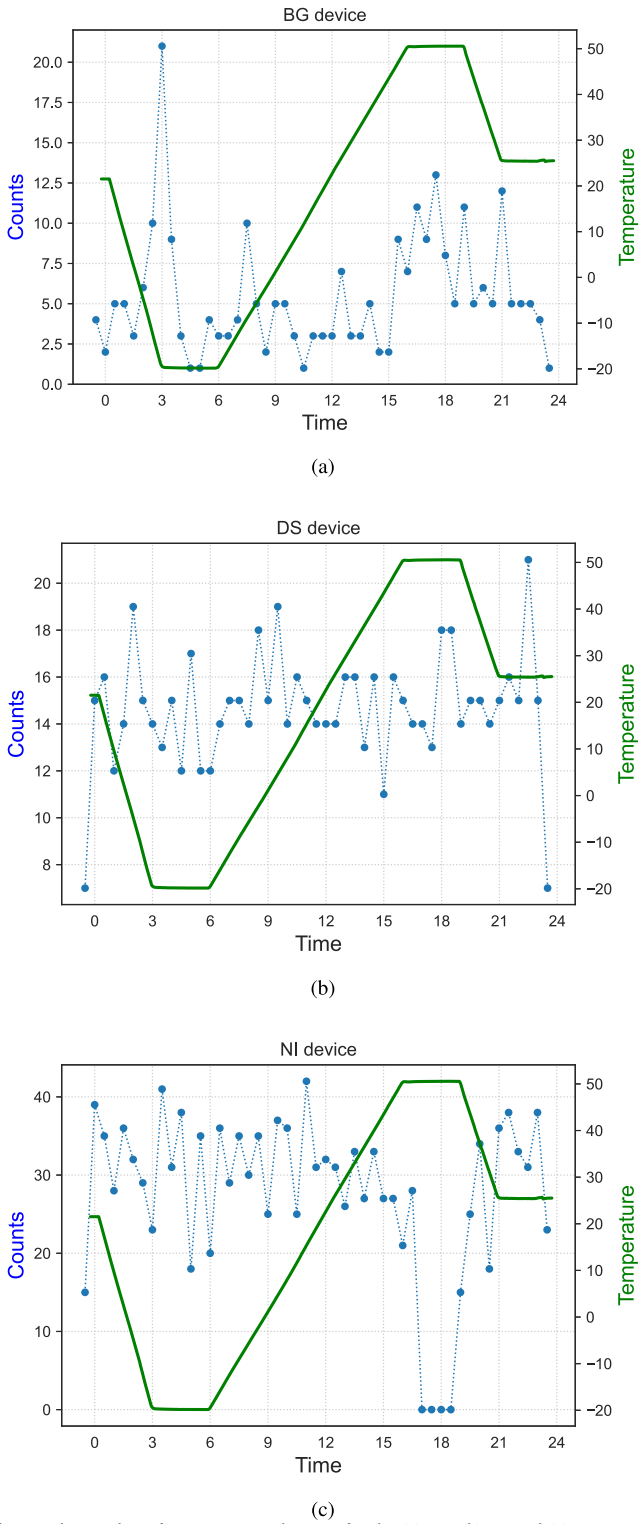

Fig. 2. The number of counts versus the time for the (a) BG, (b) DS and (c) NI sensors. The right axis (green line) shows the temperature profile followed during these tests.

Grafana while data were retrieved from the database and analyzed offline daily (see Gallego Manzano et al. (2021) for details).

Before their installation in the containers the devices were operated for several months in a laboratory, to ensure that they were working reliably and to identify possible problems that could arise before the installation. In addition, the natural background (counts per hour) as well as the alarm thresholds needed to be estimated and implemented in the firmware before deployment. In order to estimate the background, the data from all sensors were analyzed offline for several days

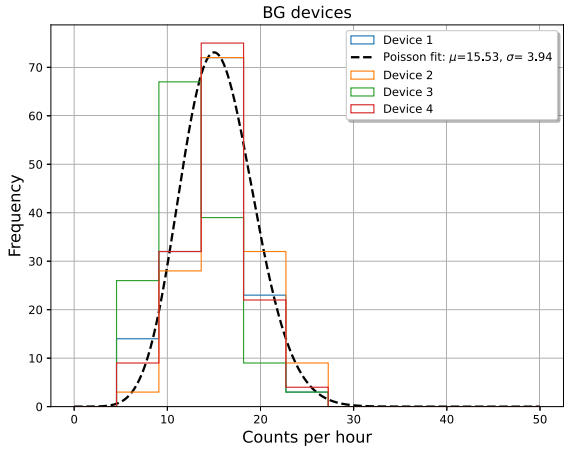

(a)

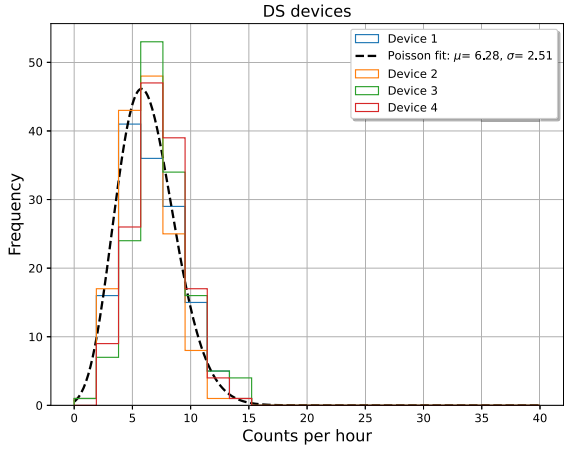

(b)

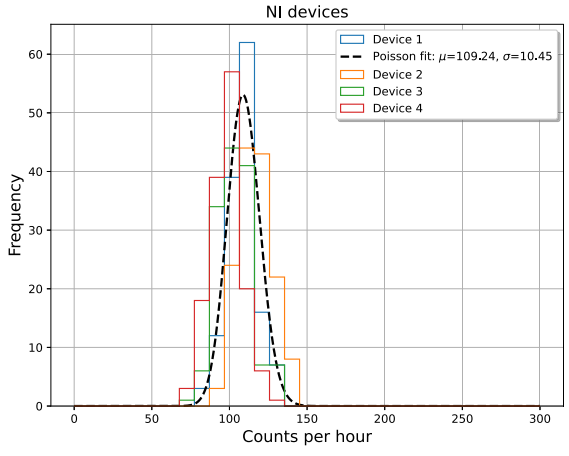

(c)

Fig. 3. Distributions of the counts per hour (cph) for four representative (a) BG, (b) DS, and (c) NI sensors. An example of a fit of a Poisson distribution to the data is also shown. The plots demonstrate that the mean expected number of counts per hour is 15, 6, and 109 for BG, DS, and NI sensors, respectively.

of continuous operation. Fig. 3 shows the background rate spectra, in counts per hour, as measured by a series of four representative sensors for each type. An example of Poisson fit to the data of the first sensor in each of the series is also shown in overlay.

The alarm threshold set in the firmware is of great importance since the device will behave in a different way if the threshold (in number of counts) is reached. If the number of counts has reached a defined threshold in a 20-min period, the device will assign a value to the alarm variable and the measurement period will no longer be one hour, as explained in Section 2.1. The firmware only supports a single identical alarm threshold that is common to all sensors of the same type. The following procedure was therefore performed to calculate the threshold for each sensor type. The distributions of the counts for each sensor were collected over a period of several days, in the absence of any radioactive source, and from each distribution the mean number of counts per hour (cph) was calculated. From that mean, the counts expected for 19 min for each sensor was deduced. From those eight means, an average value, $\bar{\mu}_{19}$ and a Poisson fluctuation uncertainty on the counts per 19 min (estimated as the square root of the average number of counts) was calculated. The standard deviation of those eight means was also calculated, in order to estimate the spread due to different sensors. The Poisson error on the average counts per 19 min and the standard deviation of the means were added in quadrature. This total uncertainty (σ) is assumed to account for both the expected Poisson fluctuation and the spread of the sensor response. To reduce the probability of a false alarm, a threshold equal to the average increased by three times the total error ($\bar{\mu}_{19} + 3\sigma$) was applied. The resulting values in counts per 19 min which were subsequently programmed in the firmware as alarm thresholds were 12 counts for BG, 7 counts for DS and 130 counts for NI.

All devices worked reliably throughout the full outdoor test period, regularly transmitting data that were received via LoRa and stored and analyzed in Grafana. These tests proved the robustness of the system in various meteorological conditions and under large temperature changes. During the monitoring and data taking period the temperature in Meyrin ranged from −2 ° C to +26 ° C, but it should be considered that the temperature inside a metallic container can raise significantly higher. There were multiple rainy, humid as well as sunny days.

4.3. Activated waste sensitivity studies

Sensitivity studies on activated waste samples were carried out using three standard containers, each equipped with eight sensors of the same type as in the on-the-field test discussed above: one with DS, one with BG and one with NI devices. The tests were performed inside the tunnel of the former Intersecting Storage Rings (ISR), which is now mostly used for radioactive waste storage. The location of the measurement was chosen at low radiation background (typically around 65–70 nSv/h) due to thick shielding walls. An indoor LoRa gateway was installed and a network was created to be able to retrieve the data, because there was no LoRa network coverage inside the tunnel. Six radioactive stainless steel samples of various size, shape, weight and activity were chosen to simulate the disposal of typical radioactive waste (Fig. 4).

At CERN, a material is considered radioactive if the net ambient dose equivalent rate, H*(10), at 10 cm distance exceeds 100 nSv/h, according to the Swiss Ordinance for Radiation Protection (Federal Office of Public Health FOPH, 2018). The dose rate of the samples was measured both at contact and at 10 cm with two different detectors: a Thermo Fischer FH40 coupled with a FHZ512 BGO probe mentioned in Section 2.2, which provides counts per second (cps); and an Automess 6150AD [10] used with a 6150AD-b scintillator probe [11], which allows fast and accurate dose rate [nSv/h] measurements down to natural background. An aspect to be considered was the non uniform distribution of radioactivity in the samples. This issue was addressed by performing measurements on all sides of the samples (see Fig. 5) and using the average value of the measurements to estimate the activity.

[10] https://www.automess.de/en/products/productfamily-6150ad/dose-rate-meter-6150ad

[11] https://www.automess.de/en/products/productfamily-6150ad/scintillator-probe

Table 1
Sample weight, total activity and net ambient dose equivalent rates H*(10) at contact/at 10 cm distance of the six activated items used in the study. The count rates of the BGO probe have been converted to H*(10) using the calibration factor of 905 cps/(μSv/h).

Sample number	Weight (g)	Total activity (kBq)	BGO count rate (cps)	BGO H*(10) (nSv/h)	6150 AD-b H*(10) (nSv/h)
1	78	1.9	173/25	191/28	170/30
2	264	3.0	279/36	308/40	288/61
3	306	60.5	3393/699	3751/773	4710/840
4	188	9.3	813/109	899/121	800/137
5	992	190.7	14123/2143	15614/2369	14640/2710
6	416	2.4	183/30	202/33	210/43

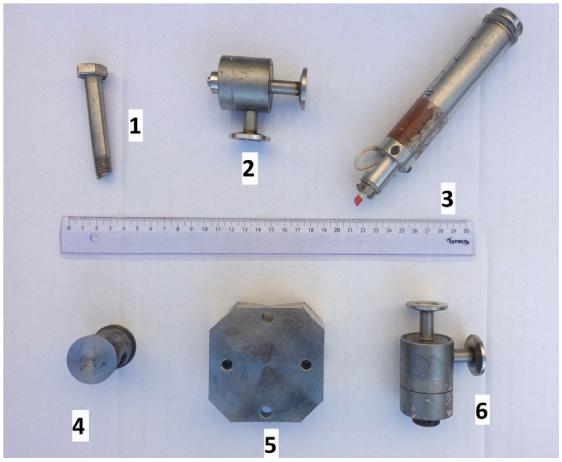

Fig. 4. The six radioactive samples used during the tests. Their size, weight and shape differ significantly.

Fig. 5. The measurement procedure with the BGO survey meter. The photo shows the measurements performed around the sample, on all its sides to take into account the non-uniformity effect which was observed. The position, angle and sample remained the same in each measurement.

The samples had dose rates at contact varying from around 0.2 μSv/h to 15 μSv/h (see Table 1).

In addition, the activity of the samples has been determined by laboratory γ-spectrometry measurements. The radionuclide present in each sample and representing the highest contributor to the total activity is Co-60. The values have a range of about 2 kBq to 190 kBq and correlate with the dose rate. The activity at the upper 2 σ confidence level is given in Table 1.

4.3.1. Precise placement test

The containers were placed in the ISR tunnel at a reasonable distance from each other and from any other material. Before starting the actual tests, the containers with the installed devices were left in place for several days to monitor the data transmission and to ensure that the background radiation level was as expected.

During the first test, the activated samples were placed in turn in the same position always in the middle of the container. The bottom half

Fig. 6. An example of how the radioactive samples were placed inside the containers, on top of the cardboard. Below the cardboard the container is filled with the PPE.

of the containers were filled with personal protective equipment, PPE (mainly plastic, paper tissues, gloves, polystyrene, etc.) to simulate the typical waste dumped in a container located just outside areas presenting a radiological risk. A sheet of cardboard was placed horizontally on top of the waste to ensure that the sample was stable and located in the center, as shown in Fig. 6.

The activated samples were put in place inside the container over a total period of nine days, but each sample for a different duration and in a random sequence. The samples were placed by the technicians working on site without informing the analyzing team. This "blind" technique in terms of exposure time and level of activity removed any prior knowledge of the procedure that could create a bias in the analysis of the results.

The results are shown in Tables 2–4 for the three containers equipped with BG, DS and NI devices respectively: sample, duration of exposure and whether the sample has been detected or not by the W-MON system and by the standard manual search using the BGO survey meter. It should be mentioned that with the manual search procedure, the technician does not only perform a measurement outside the container, but he/she also opens the lid and place the BGO probe inside the container, before concluding that it is radiation free or not.

The data from the measurements were transmitted via LoRa and finally shown in the monitoring tool implemented with Grafana. The analysis was performed offline with the data retrieved from influxDB and analyzed without any information from the online monitoring. The data were analyzed without any prior knowledge or access to Grafana. However, after the data were evaluated and the results finalized, they could also be viewed on Grafana as shown in Fig. 7.

Fig. 7 shows the measured rate in counts per hour (cph) after dividing the number of counts with the actual integration time (measured in seconds) and scaling by 3600 s:

$$\text{Normalized Rate} = \frac{\text{counts per interval} \cdot 3600\ \text{s}}{\text{integration time}} \tag{3}$$

The actual integration time is 3420 s or 57 min since 3 min are used for the initialization and preparation of the measurement periods.

Fig. 7. Monitoring tool output showing the normalized rate for the period of the precise placement tests for BG, DS and NI devices respectively. Each subfigure shows the eight devices used in different colors. Notice that some of the samples were undoubtedly detected by the W-MON system while other samples with lower activity were not able to trigger the alarm by exceeding the threshold. Tables 2–4 show the detailed results.

Table 2
Results of the precise placement test for the container equipped with the BG devices.

Sample number	Duration of exposure (h)	Detected by W-MON	Detected by BGO
3	21	Yes	Yes
6	72	No	No
2	25	No	No
5	18	Yes	Yes
3	17	Yes	Yes
5	7	Yes	Yes
4	17	Yes	No
3	6	Yes	Yes

Table 3
Results of the precise placement test for the container equipped with the DS devices.

Sample number	Duration of exposure (h)	Detected by W-MON	Detected by BGO
2	21	Yes	No
3	72	Yes	Yes
6	44	No	No
6	17	No	No
3	7	Yes	Yes
5	17	Yes	Yes
4	6	Yes	No

Table 4
Results of the precise placement test for the container equipped with the NI devices.

Sample number	Duration of exposure (h)	Detected by W-MON	Detected by BGO
6	21	No	No
2	72	No	No
3	44	Yes	Yes
5	17	Yes	Yes
4	7	Yes	No
3	17	Yes	Yes
5	6	Yes	Yes

Table 5
Results of the random placement test for the container equipped with the BG devices.

Sample number	Duration of exposure (h)	Detected by W-MON	Detected by BGO
3	18	Yes	Yes
4	7	Yes	Yes
2	17	No	Yes
1	17	No	Yes
6	9	Yes	No
5	15	Yes	Yes

Table 6
Results of the random placement test for the container equipped with the DS devices.

Sample number	Duration of exposure (h)	Detected by W-MON	Detected by BGO
2	18	No	Yes
3	7	Yes	Yes
4	17	Yes	Yes
6	7	Yes	Yes
1	9	No	Yes
5	9	Yes	Yes

4.3.2. Random placement test

During this test the containers were completely filled with PPE waste, and the radioactive samples were thrown randomly inside over a period of six days, for different periods of time and in various order (Fig. 8).

Table 7
Results of the random placement test for the container equipped with the NI devices.

Sample number	Duration of exposure (h)	Detected by W-MON	Detected by BGO
4	18	Yes	Yes
2	7	Yes	Yes
3	17	Yes	Yes
1	7	No	Yes
6	17	Yes	Yes
5	15	Yes	Yes

Fig. 8. Radioactive sample placed randomly in a container filled with ordinary waste.

As before, this blind technique was adopted to remove any possible bias in the analysis. As for the test described in the previous section, the data were analyzed offline to verify the sensitivity of the W-MON system and to conclude if each configuration was detectable by W-MON and by the manual procedure. Tables 5–7 summarize the results for the three containers equipped with the BG, DS and NI devices, with the same format as above. Fig. 9 shows the Grafana monitoring system view after the data were evaluated.

5. Conclusions

The W-MON demonstration system discussed in this paper consists of a network of IoT devices equipped with radiation sensors designed to detect and alert for the presence of radioactive material in containers for ordinary waste. The network was implemented using the LoRaWAN technology, allowing wide area coverage, low-power consumption and minimal servicing of the devices over long periods of time. Three different radiation sensors were tested in combination with a common custom-built communication board with specialized firmware. Commercial technologies such as InfluxDB and Grafana were used to implement the collection, storing, analysis, monitoring and visualization of the data. After the radiation sensors were calibrated in the CERN Radiation Calibration Laboratory, extended tests were performed first in a laboratory and then in operational conditions to ensure that the devices can withstand the environmental conditions expected when used on the waste bins. Subsequently, the devices were submitted to field tests with samples of activated materials typically encountered in CERN radiological areas. In real-world conditions, these tests demonstrated that W-MON can detect activated material discarded in containers relatively early and reliably without manual intervention, as long as its activity is high enough. The level of detection was slightly better than with the conventional radiological measuring devices. At the same time, the system has the added benefits of registering the time

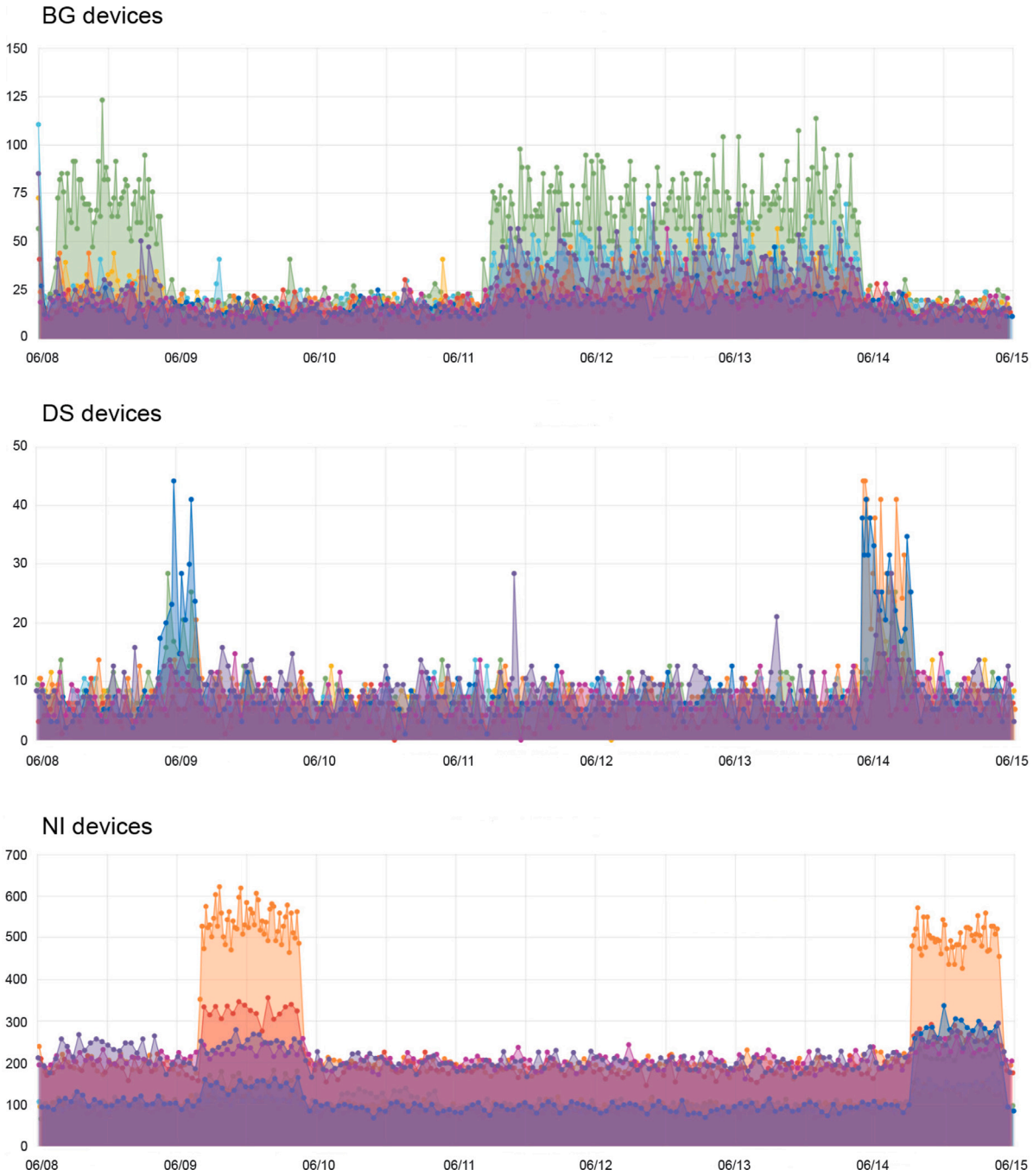

Fig. 9. Monitoring tool output showing the normalized rate for the period of the random placement tests for BG, DS and NI devices respectively. Each subfigure shows the eight devices used in different colors. We notice that some of the samples were undoubtedly detected by the W-MON system while other samples with lower activity were not able to set the alarm by surpassing the threshold. These samples were mostly samples 1 and 2. Tables 5–7 show the detailed results.

of the event and storing the data in a database for further analysis. Finally, the system eliminates the variability and reliability issues introduced by a human operator.

CRediT authorship contribution statement

N. Heracleous: Conceptualization, Data curation, Formal analysis, Funding acquisition, Investigation, Methodology, Project administration, Resources, Software, Supervision, Validation, Visualization, Writing – original draft, Writing – review & editing. **K. Bauer:** Investigation, Resources, Validation, Writing – original draft, Writing – review & editing. **L. Gallego Manzano:** Formal analysis, Methodology, Resources, Software, Validation, Writing – original draft, Writing – review & editing. **F. Murtas:** Conceptualization, Data curation, Formal analysis, Investigation, Methodology, Resources, Software, Supervision, Validation, Visualization. **M. Silari:** Conceptualization, Formal analysis, Funding acquisition, Investigation, Methodology, Project administration, Resources, Supervision, Validation, Writing – original draft, Writing – review & editing. **L. Svihrova:** Investigation, Resources, Validation, Writing – review & editing.

Declaration of competing interest

The authors declare that they have no known competing financial interests or personal relationships that could have appeared to influence the work reported in this paper.

Data availability

Data will be made available on request.

Acknowledgments

This work would not have been possible without the precious involvement and dedication of Fabrizio Murtas who passed away before the results were documented. We would also like to thank various colleagues around CERN, especially from the IT-CS-TR section for the LoRa network, the IT-DA-DS section for the data streaming and visualization tools, the BE-CEM-EPR section for the intermediate board and firmware, the HSE-RP-IL section for the fruitful discussions and advice on electronics and board design as well as collaborators from CERAP and FOSELEV for the operational handling of the samples and measurements.

References

Cattani, M., Boano, C.-A., Römer, K., 2017. An experimental evaluation of the reliability of LoRa long-range low-power wireless communication. J. Sensor Actuator Netw. http://dx.doi.org/10.3390/jsan6020007.

Federal Office of Public Health FOPH, 2018. Radiological Protection Ordinance. SR 814.501, Swiss Federal Council.

Gallego Manzano, L., Bisegni, C., Boukabache, H., Curioni, A., Heracleous, N., Murtas, F., Perrin, D., Silari, M., 2020. A distributed and interconnected network of sensors for environmental radiological monitoring. Radiat. Meas. 139, 106488. http://dx.doi.org/10.1016/j.radmeas.2020.106488, URL https://www.sciencedirect.com/science/article/pii/S1350448720302626.

Gallego Manzano, L., Boukabache, H., Danzeca, S., Heracleous, N., Murtas, F., Perrin, D., Pirc, V., Alfaro, A.R., Zimmaro, A., Silari, M., 2021. An IoT LoRaWAN network for environmental radiation monitoring. IEEE Trans. Instrum. Meas. 70, 1–12. http://dx.doi.org/10.1109/TIM.2021.3089776.

Ledeul, A., Segura, G., Silvola, R.-P., Styczen, B., Vasques Ribeira, D., 2015. REMUS: The new CERN radiation and environment monitoring unified supervision. In: 15th International Conference on Accelerator and Large Experimental Physics Control Systems. p. TUD3O03. http://dx.doi.org/10.18429/JACoW-ICALEPCS2015-TUD3O03.

Van Rossum, G., Drake, F.L., 2009. Python 3 Reference Manual. CreateSpace, Scotts Valley, CA.

Wennerström, H., Hermans, F., Rensfelt, O., Rohner, C., Nordén, L.-A., 2013. A long-term study of correlations between meteorological conditions and 802.15.4 link performance. In: 2013 IEEE International Conference on Sensing, Communications and Networking. SECON, pp. 221–229. http://dx.doi.org/10.1109/SAHCN.2013.6644981.